



HAL
open science

THE DETECTION OF A POTENTIAL BIOSIGNATURE BY THE PERSEVERANCE ROVER ON MARS

Joel A. Hurowitz, Michael M. Tice, Abigail C. Allwood, Morgan L. Cable,
Kevin P Hand, A. E. Murphy, K. Uckert, James F Bell, Tanja Bosak, Adrian
Broz, et al.

► **To cite this version:**

Joel A. Hurowitz, Michael M. Tice, Abigail C. Allwood, Morgan L. Cable, Kevin P Hand, et al..
THE DETECTION OF A POTENTIAL BIOSIGNATURE BY THE PERSEVERANCE ROVER
ON MARS. 56th Lunar and Planetary Science Conference, Lunar and Planetary Institute, Mar 2025,
The Woodlands (Texas), United States. pp.2581. hal-04930754

HAL Id: hal-04930754

<https://hal.science/hal-04930754v1>

Submitted on 5 Feb 2025

HAL is a multi-disciplinary open access archive for the deposit and dissemination of scientific research documents, whether they are published or not. The documents may come from teaching and research institutions in France or abroad, or from public or private research centers.

L'archive ouverte pluridisciplinaire **HAL**, est destinée au dépôt et à la diffusion de documents scientifiques de niveau recherche, publiés ou non, émanant des établissements d'enseignement et de recherche français ou étrangers, des laboratoires publics ou privés.

THE DETECTION OF A POTENTIAL BIOSIGNATURE BY THE *PERSEVERANCE* ROVER ON MARS.

J.A. Hurowitz¹, M.M. Tice², A.C. Allwood³, M.L. Cable³, K.P. Hand³, A.E. Murphy⁴, K. Uckert³, J.F. Bell III⁵, T. Bosak⁶, A.P. Broz⁷, E. Clave⁸, A. Cousin⁹, S. Davidoff³, E. Dehouck¹¹, K.A. Farley¹², S. Gupta¹³, S-E Hamran¹⁴, K. Hickman-Lewis^{13,15}, J.R. Johnson¹⁶, P.S. Jørgensen¹⁷, L.C. Kah¹⁸, H. Kalucha¹², T.V. Kizovski^{19,20}, D.A. Klevang-Pedersen¹⁷, Y. Liu³, F. M. McCubbin²¹, E.L. Moreland²², G. Paar²³, D.A. Paige²⁴, A.C. Pascuzzo²⁵, M. S. Rice²⁶, M.E. Schmidt²⁰, K.L. Siebach²², S. Siljeström²⁷, J.I. Simon²¹, K.M. Stack³, A. Steele²⁸, N.J. Tosca²⁹, A.H. Treiman³⁰, S.J. VanBommel³¹, L.A. Wade³, B.P. Weiss⁶, R.C. Wiens⁷, K.H. Williford³², R. Barnes¹³, P.A. Barr²⁵, A. Bechtold³³, P. Beck³⁴, K. Benzerara³⁵, S. Bernard³⁵, O. Beyssac³⁵, R. Bhartia³⁶, A.J. Brown³⁷, G. Caravaca^{9,38}, E.L. Cardarelli²⁴, E.A. Cloutis³⁹, A.G. Fairén^{40,41}, D.T. Flannery⁴², T. Fornaro⁴³, T. Fouchet⁴⁴, B. Garczyski²⁶, F. Gómez⁴⁰, E.M. Hausrath⁴⁵, C.M. Heirwegh³, C.D.K. Herd⁴⁶, J.E. Huggett²⁵, A.J. Jones^{13,47}, M.W.M. Jones, J.L. Jørgensen¹⁷, A.Y. Li⁴⁸, J.N. Maki³, L. Mandon³⁴, N. Mangold⁴⁹, J.A. Manrique-Martinez⁵⁰, J. Martínez-Frias⁵¹, J. I. Núñez¹⁶, L.P. O'Neil², B.J. Orenstein⁴², C. Quantin-Nataf¹¹, P. Russell²⁴, M.D. Schulte⁵², S. Sharma²⁸, D.L. Shuster⁵³, A. Srivastava²⁸, B.V. Wogsland¹⁸, Z.U. Wolf⁵⁴. ¹Stony Brook University, joel.hurowitz@stonybrook.edu, ²Texas A&M University, ³Jet Propulsion Laboratory, ⁴Planetary Science Institute, ⁵Arizona State University, ⁶Massachusetts Institute of Technology, ⁷Purdue University, ⁸DLR Institute of Optical Sensor Systems, ⁹IRAP, Université Paul Sabatier Toulouse, ¹¹Université Claude Bernard Lyon, ¹²California Institute of Technology, ¹³Imperial College London, ¹⁴University of Oslo, ¹⁵University of London, ¹⁶Johns Hopkins University Applied Physics Laboratory, ¹⁷Technical University of Denmark, ¹⁸University of Tennessee, ¹⁹Royal Ontario Museum, ²⁰Brock University, ²¹NASA Johnson Space Center, ²²Rice University, ²³Joanneum Research, Institute for Information Technologies, ²⁴University of California, Los Angeles, ²⁵Malin Space Science Systems, ²⁶Western Washington University, ²⁷RISE Research Institutes of Sweden, ²⁸Carnegie Science Earth & Planets Laboratory, ²⁹University of Cambridge, ³⁰Lunar and Planetary Institute, ³¹Washington University in St. Louis, ³²Blue Marble Space Institute of Science, ³³Austrian Academy of Sciences, ³⁴Université Grenoble Alpes, ³⁵IMPMC, Sorbonne Université, Museum National d'Histoire Naturelle, ³⁶Photon Systems, Inc., ³⁷Plancius Research, ³⁸GET, Université Paul Sabatier Toulouse III, ³⁹University of Winnipeg, ⁴⁰Centro de Astrobiología, CSIC-INTA, ⁴¹Cornell University, ⁴²School of Earth and Atmospheric Sciences, Queensland University, ⁴³INAF-Astrophysical Observatory of Arcetri, ⁴⁴LESIA, Observatoire de Paris, Université PSL, CNRS, Sorbonne Université, Université Paris Cité, ⁴⁵University of Nevada-Las Vegas, ⁴⁶University of Alberta, ⁴⁷School of Chemistry and Physics, Central Analytical Research Facility, Queensland University of Technology, ⁴⁸University of Washington, ⁴⁹LPG, CNRS, Nantes Université, ⁵⁰University of Valladolid, ⁵¹Institute of Geosciences, CSIC-UCM, ⁵²NASA Headquarters, ⁵³University of California, Berkeley, ⁵⁴LANL.

Introduction: The *Perseverance* rover has explored and sampled igneous and sedimentary rocks in Jezero crater to characterize early Martian geological processes and habitability and search for biosignatures. Upon entering Neretva Vallis, *Perseverance* investigated a set of distinct mudstone and conglomerate outcrops. We report on measurements from these rocks and describe the discovery of a potential biosignature [1].

Geologic Context: Neretva Vallis incises the Jezero crater rim and its Margin Unit; it was the feeder channel for the Western Fan sedimentary deposit [2]. *Perseverance* explored a set of outcrops exposed along its northern contact with the Margin Unit. In HiRISE images of this deposit, albedo variations appeared to indicate layering at the meter scale. Subsequently, *Perseverance* explored strata along the southern margin of Neretva Vallis, where rocks with similar characteristics in orbital images crop out. Collectively, these outcrops are called the Bright Angel formation.

The Bright Angel formation consists of ~meter-scale blocks formed by fracturing and physical weathering of the exposed outcrop. Rock textures include laminated, layered, and structureless intervals

with limited indications of deposition or reworking by currents, such as cross bedding or plane bed laminations [3]. In the outcrops along the southern margin of Neretva Vallis, poorly sorted matrix-supported conglomerates are also observed [3].

Petrographic Relationships: Rocks investigated in the Bright Angel formation are dominated by a fine-grained facies that comprises much of the rock volume. It is composed of grains $\leq \sim 30\text{-}110\ \mu\text{m}$ diameter. We classify this facies as mudstone. Bright Angel conglomerates contain a matrix made of the same mudstone, as well as mm- to cm-scale clasts, often composed of mudstone and representing intraclasts.

The mud facies exhibits visible light reflectance properties in spectra collected by the Mastcam-Z and SuperCam instruments that indicate variable abundances of ferric iron, resulting in color properties that range from red, to tan, to whitish-gray. PIXL micro-XRF elemental analyses indicate that Bright Angel formation mudstones are uniformly SiO₂, Al₂O₃, and FeO rich, and MgO and MnO poor, implying abundant silica, aluminosilicate clays, and Fe-oxides. In Bright Angel formation targets on the northern side of Neretva Vallis, organic matter was detected by the

SHERLOC instrument based on the presence of a 1600 cm^{-1} G-band in Raman spectra [4]. No G-band was detected in targets from southern Neretva Vallis.

Dispersed throughout the fine-grained mudstone facies of all targets analyzed on the northern side of Neretva Vallis, we observe $\sim 100\text{-}200\ \mu\text{m}$ circular to irregularly shaped masses that are black to dark blue to dark green colored. These features are informally called ‘Poppy Seeds’. A striking feature observed in the Cheyava Falls target is distinct spots that have circular to crenulated dark-toned rims and lighter toned cores. These spots range in size from $\sim 200\ \mu\text{m}$ to 1 mm in diameter and their cores are less red than the mudstone that surrounds their rims. Like the poppy seeds they co-occur with (Fig. 1A), the spots do not appear to be concentrated in layers or laminae, indicating that they were not deposited as grains. Instead, they appear to represent in-situ reaction fronts. These features are informally named ‘Leopard Spots’. PIXL analysis reveals that poppy seeds and leopard spot rims are enriched in ferrous iron and phosphorous, while leopard spot cores are enriched in iron and sulfur (Fig. 1B). These enrichments are interpreted to reflect the presence of vivianite and greigite, respectively.

Synthesis: Available outcrop and petrographic-scale observations lead us to conclude that the Bright Angel formation was formed by deposition from mud-dominated suspension and mass flow. Facies associations are consistent with a valley-confined lacustrine setting [3]. The sediment that makes up the Bright Angel formation was generated by chemical weathering under oxidizing conditions in the sediment source region. After deposition, early diagenetic redox reactions generated the poppy seeds and leopard spots.

Poppy seeds and leopard spots co-occur with organic carbon in ferric-iron poor mudstones but are absent in ferric iron-rich mudstones and conglomerates that lack organic matter (Fig. 1C). These relationships indicate the vivianite and greigite in these features formed by reaction between organic matter, oxidized iron, and sulfate; geological context and petrography indicate these reactions occurred at low temperatures. On Earth, such organic matter mediated mineral forming reactions are often driven by, or are closely associated with, microbial respiration of organic matter [e.g., 5], and models of the reaction chemistry that formed these features are consistent with microbially mediated process [6]. These properties mark poppy seeds and leopard spots as *potential* biosignatures. Analysis of the core sample collected from this unit using high-sensitivity instrumentation on Earth will enable tests to assess the biogenicity of the minerals, organics, and textures it contains.

References: [1] Hurowitz, J. et al., submitted; [2] Goudge, T. et al., 2015, *JGR-P*; [3] Jones, A. et al., 56th LPSC; [4] Murphy A., et al., 56th LPSC; [5]

Frankel, R. and Bazylinski, D., 2003, *RiMG*, 54(1); [6] Tice, M. et al., 56th LPSC.

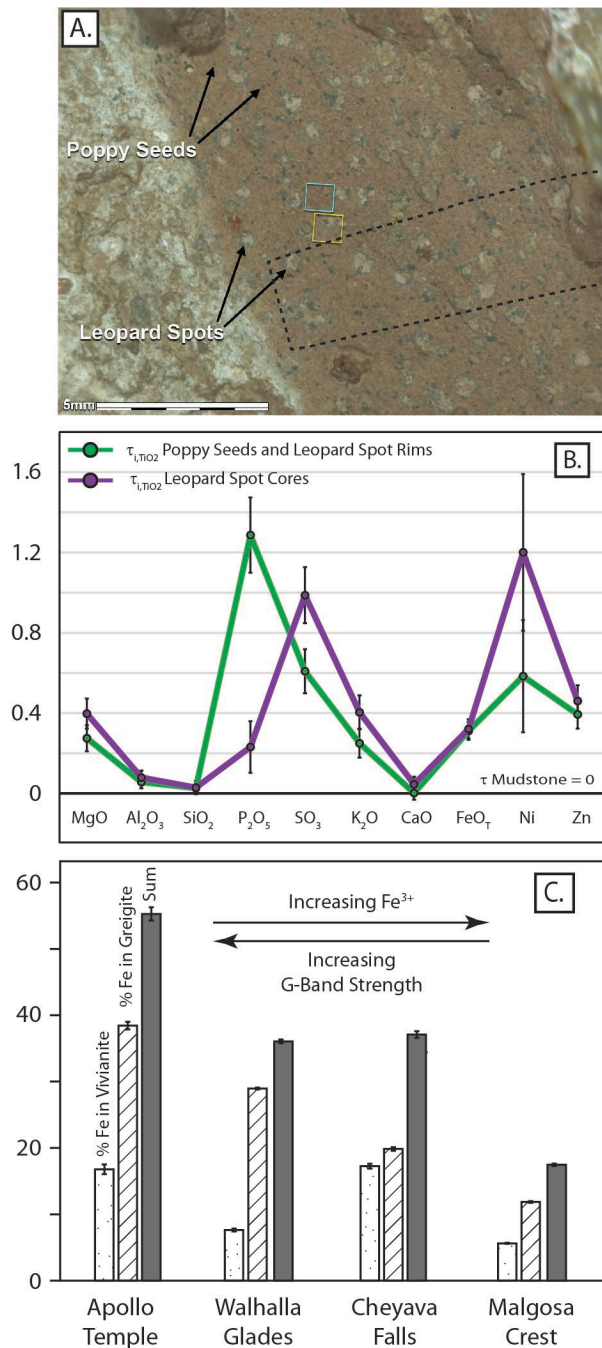


Fig. 1: (A) Colorized ACI image of the target Cheyava Falls, poppy seeds and leopard spots. PIXL (black dashed rectangle) and SHERLOC scan areas (blue and orange squares) overlain. (B) Element mobility index for the indicated elements showing enrichment and depletion patterns for poppy seeds and leopard spot rims (green) and leopard spot cores (purple) relative their host mudstone. (C) Maximum % total iron in each Bright Angel target that could be present as vivianite, greigite, and their sum, and their relationship to ferric iron and organic matter detections.